PHILOSOPHICAL MAGAZINE B, 1986, VOL. 54, NO. 1, 51 60

Electron drift mobility in amorphous Si:H

By J. M. MARSHALL

Department of Physics, Dundee College of Technology,
Bell Street, Dundee DD1 1HG, Scotland

R. A. STREET and M. J. THOMPSON

Xerox Palo Alto Research Centre, Palo Alto, California 94304, U.S.A.

[*Received 7 February 1986 and accepted 24 February 1986*]

ABSTRACT

The 'time of flight' technique has been employed to study the transient photoconductivity due to excess electron carriers in amorphous Si:H, over a wide range of temperature and electric field. The data are analysed in terms of the temperature/field dependence of the carrier transit time, and also in terms of the variation in pulse shape with temperature. In both cases, the behaviour suggests interactions with a tail of states extending about 0·15 eV from the band edge and showing an almost linear variation of trap density with energy over at least the range 0·085 to 0·145 eV. The capture cross-section of the centres is estimated to be of order 10^{-17}–10^{-16} cm^2. Interaction with states beyond the tail is comparatively weak, and is dominated by deep trapping into centres believed to be dangling bonds.

§ 1. INTRODUCTION

Over the past decade, considerable attention has been directed towards the study of charge-carrier transport processes in hydrogenated amorphous silicon, as prepared by the glow-discharge decomposition of silane gas. It is, therefore, rather surprising that the characterization of electron transit pulses obtained using the 'time of flight' technique remains fragmentary. Although various room-temperature measurements have been reported for relatively low values of electric field, only a restricted amount of information exists concerning the behaviour over a broader range of temperature and field. This represents a serious limitation, since such data are potentially of considerable value in the identification of the energy distribution and nature of localized states below the mobility edge, as well as the mobility of free carriers beyond the edge.

At room temperature, electron transit pulses approach a conventional form (Tiedje, Cebulka, Morel and Abeles 1981, Spear 1983, Marshall, Street and Thompson 1984 a, b, Marshall, Le Comber and Spear 1985), as opposed to displaying the 'anomalously dispersive' character which has been extensively studied over recent years (see Marshall (1983) for a review). The spread of individual carrier transit times indicated by the falling edge of the pulse is rather larger than would be expected from conventional diffusion theory, but this (at least in part) probably reflects the anomalous broadening of the carrier packet in the first nanosecond or so, during which period carriers approach quasi-thermal equilibrium with shallow trapping centres.

The temperature dependence of the carrier mobility has been studied by Tiedje *et al.* (1981), Marshall *et al.* (1984 a, b), Spear and Steemers (1984) and Hourd and Spear

(1985), and has been found to be of activated form below about 300 K. A low-field activation energy of 0·14 eV or more is found, with smaller energy values tending to be observed in more recent studies, as material quality has improved. Above 300 K, the mobility increases less rapidly, and high-temperature saturation values of order $10\,cm^2\,V^{-1}\,s^{-1}$ have been inferred (see below).

Although transit pulses assume a conventional form at the higher end of the temperature range, the dispersion increases upon cooling, and becomes quite appreciable below about 200 K (Tiedje *et al.* 1981, Tiedje 1984, Marshall *et al.* 1984 a, b). A similar phenomenon has been observed in the case of other disordered semiconductors and has been demonstrated to be consistent with a mechanism of trap-limited transport, in which the controlling centres are distributed over at least a few kT in energy (Marshall 1983).

Whilst previous studies have provided a basic identification of the trap-limited transport mechanism, it is clear that a detailed interpretation requires further data covering a wide range of temperature and field. This is particularly the case since attempts are being made to estimate the energy distribution of localized states from such data (for example, Davis, Michiel and Adriaenssens (1985)).

In the present paper, we report measurements taken over the temperature range 100–350 K, and (where accessible) the field range 5×10^2–$5 \times 10^4\,V\,cm^{-1}$. Thereby, we cover a much broader spectrum of conditions than in previous studies; providing data suitable for a detailed computation of the energy distribution of localized states below the conduction band.

§ 2. Experimental details

The material used in the investigation was produced via the plasma decomposition of SiH_4, as described elsewhere (Street, Knights and Biegelsen 1978). The specimen chosen for detailed examination in the present study was typical of the better quality material produced in the Xerox Palo Alto laboratories, showing good room-temperature electron mobility and lifetime. The measurements were performed using a conventional 'time of flight' system (Spear 1968, Street 1982).

As in previous studies, transit pulses became increasingly dispersive as the temperature fell. To assist in the identification of a transit time under anomalously dispersive conditions, the technique of combining pulses taken for differing fields (Marshall and Allen 1979, Marshall *et al.* 1984 b) was adopted. Figure 1 displays such data for the various temperatures and fields investigated. The transition to extraction-dominated behaviour is readily established from such combined curves, and transit times (arrows in fig. 1) were taken as the points at which 20% of the carriers had completed their transits, as identified by a corresponding fall in current relative to the extraction-free characteristic. The resulting mobilities are therefore those of the *fastest* carriers, crossing the specimen at the leading edge of the carrier packet (as opposed to an *average* mobility of the excess carriers). To avoid confusion, the above technique was retained even for the 'normally dispersive' pulses obtained at high temperatures (thereby yielding mobility values about 30–50% higher than the *average* drift mobility in this regime). Values of transit time determined using the above procedure will be comparable, to a reasonable approximation, with those evaluated by the technique employed in some previous studies, in which power-law characteristics are force-fitted to the initial and final regimes (Pfister and Scher 1978). However, the present procedure makes it unnecessary to use such assumptions, and allows an identification of the transit time even where pulse shapes are not well described by the power-law model.

Fig. 1

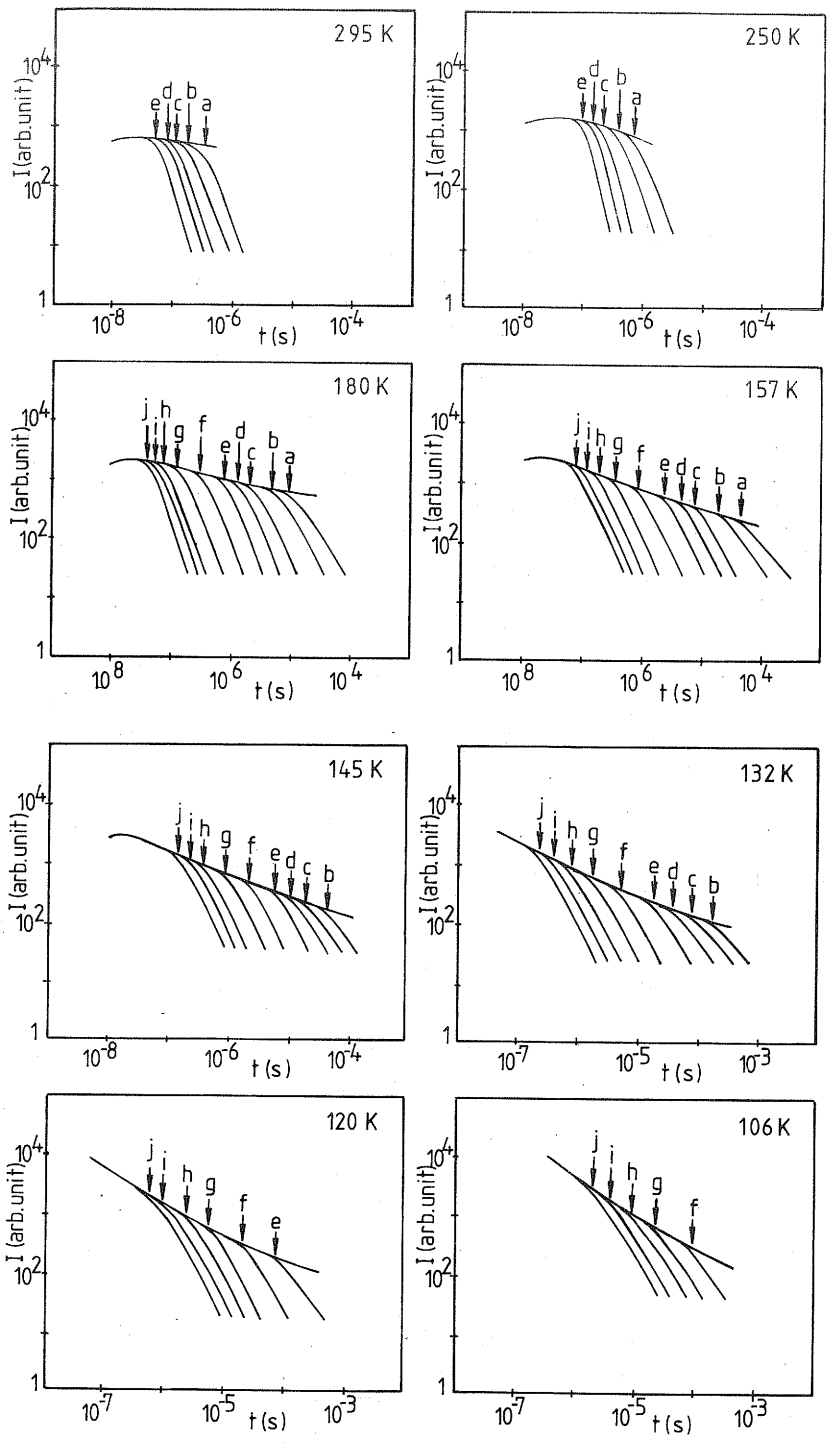

Electron time-of-flight photoresponse characteristics for a range of temperatures, and for electric fields (kV cm^{-1}) as follows: *a*, 0·5; *b*, 1; *c*, 2; *d*, 3; *e*, 5; *f*, 10; *g*, 20; *h*, 30; *i*, 40; *j*, 50.

Fig. 2

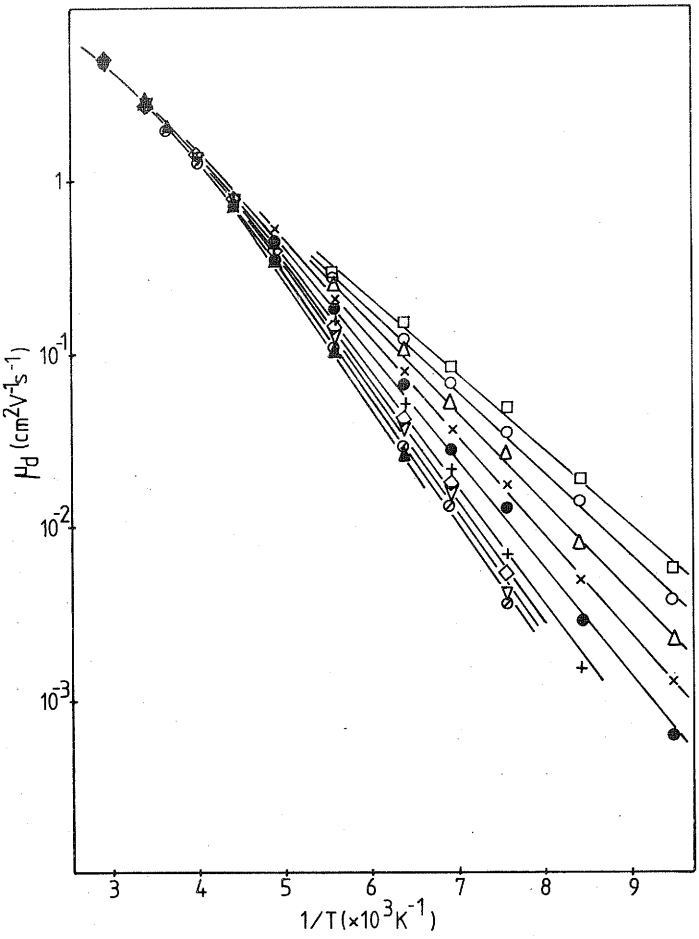

Temperature dependence of the electron drift mobility for various values of applied electric field.

Figure 2 displays the temperature dependence of the mobility for various values of applied field. At the higher temperatures, it was necessary to restrict the range of field, since high-field transit times approached the resolution of the detection system. As we shall show, the energy distribution of localized states may be estimated from the field dependence of the drift mobility and of its activation energy. The table summarizes the activation energy values for the low-temperature data of fig. 2, and also contains values of trap density and capture cross-section, computed as described below.

§ 3. Discussion

3.1. *Temperature dependence of the low-field mobility*

Below about 220 K, the drift mobility measured at the lowest accessible fields is singly activated, with an activation energy close to 0·14 eV. Taking free-carrier transport to be via extended states in the conduction band, a straightforward interpretation of such behaviour is that electrons undergo interactions with localized states, and that such interactions are dominated by centres located about 0·14 eV below

Activation energies, trap densities and capture cross-section (see fig. 2).

Symbol	F (kV cm^{-1})	E_m (eV)	$N(E_m)$ (rel.) (eqn. 4)	$N(E_m)$ (rel.) (eqn. 5)	$N(E_m)/N_c$ (eqn. 1)	σ (10^{-17} cm^{-2})
□	50	0·086	5	4·6	0·17	1·0
○	40	0·093	4	3·8	0·13	1·1
△	30	0·103	3	3·5	0·076	1·4
×	20	0·113	2	3·25	0·045	1·5
●	10	0·122	1	2·5	0·030	1·2
+	5	0·132	0·5	1·6	0·019	1·0
◇	3	0·137	0·3	1·4	0·016	0·7
▽	2	0·140	0·2	1·1	0·014	0·5
∅	1	0·142	0·1	0·85	0·014	0·3
▲	0·5	0·145	0·05	0·67	0·013	0·14

the mobility edge. For such a model, one expects (Rose 1951) deviations from activated behaviour at higher temperatures, as the mobility approaches its extended state value μ_0:

$$\mu = \mu_0/(1 + [N_t/N_c] \exp(E/kT)) \rightarrow \mu_0 \text{ as } T \rightarrow \text{infinity}, \quad (1)$$

where N_c and N_t are respectively the effective densities of states at the mobility edge and close to a depth $E \sim 0{\cdot}14$ eV. The best fit of the low-field experimental data to eqn. (1) indicates a free-carrier mobility of about 20 cm^{-2} V^{-1} s^{-1}, and a ratio N_t/N_c of order 10^{-2}. Comparable values have been obtained by Hourd and Spear (1985), using a basically similar model with certain refinements. Tiedje *et al.* (1981) estimated a free mobility of 13 cm^2 V^{-1} s^{-1} assuming an *exponential* tail of localized states, possibly suggesting that the value may be relatively insensitive to the fine detail of the model employed. However, recent studies by Michiel, Davis and Adriaenssens (1985) have called into question the ability of the exponential-tail model to fit the experimental data, and have suggested rather larger free-carrier mobilities (of order 50 cm^2 V^{-1} s^{-1}).

In the case of an *amorphous* semiconductor, although centres associated with a particular species of defect may exist, it is not generally believed that these will all have the same release energy. Rather, it is anticipated that defect states in the mobility gap will be disorder-broadened to a greater or lesser extent. Also, tails of localized states will project from the band edges by perhaps a few tenths of an eV (Mott 1969). Ballistic considerations of capture into, and release from, these energetically-distributed states during a carrier's transit of the specimen, determine the detailed nature of the transient response. Consequently, a thorough study of the influence of field and temperature upon pulse shape and transit time is capable of providing information concerning the nature and energy distribution of the centres with which carriers interact. In particular, we immediately note the weakness of the field dependence of the mobility at low (5–50×10^2 V cm^{-1}) fields. Reducing the field by a factor of ten produces a proportionate increase in the free-carrier transit time, and thus of the time available for capture into deeper states. The fact that the mobility activation energy increases only slightly indicates a rather abrupt change in the energy distribution and/or nature of states close to the 0·14 eV level. We shall return to this aspect of the behaviour, and to a more quantitative assessment of the energy distribution, at a later stage.

3.2. *Transit pulse shape in the high-temperature regime*

Although there is no abrupt transition between the high-T and low-T forms of the transient response, it is clear that above about 250 K the pulses approach a conventional form. They commence with a (presumed) rapid fall in current as initially free carriers interact with traps (not resolved with the present equipment, which has a rise time of order 10 ns), followed by a region in which the current is almost constant until carriers begin to reach the extinction electrode. The persistence of such a plateau from a time of 10 ns (or less) to over 100 ns constitutes further evidence that, once carriers have approached quasi-thermal equilibrium with shallow tail states, their interaction with deeper centres is distinctly limited (Marshall *et al.* 1985). A lifetime for trapping into such 'deep' states may be estimated by studying the completeness of charge collection. For the present specimen and for other similarly prepared material, a value of order 10^{-6} s is obtained (Street, Zesch and Thompson 1983).

We note that the rather qualitative distinction between 'deep' and 'shallow' traps which has been presented above may be given a more formal basis in terms of carrier ballistics, as established elsewhere (Marshall 1985).

3.3. *The low-temperature regime and high-field characteristics*

Below about 200 K, transit pulses become quite markedly anomalous in form, and at temperatures approaching 100 K the dispersion becomes sufficient to prevent identification of transit times, even using the decay-curve combination procedure. As previously indicated, the anomalous behaviour reflects the (incomplete) process of thermalization of carriers with energetically distributed traps, and thereby provides information concerning the energy distribution of such states. Note that the tendency towards a conventional degree of dispersion at high temperatures is by no means inconsistent with the above interpretation, since at such temperatures the energy distribution of shallow-trapped excess carriers approaches its quasi-thermal equilibrium value much more rapidly.

Given the general decrease in mobility with falling temperature, it becomes feasible to study the characteristics over a wide range (5×10^2–5×10^4 V cm^{-1}) of electric field. Under *highly dispersive* conditions, the measured transit time is approximately equal to the release time constant of the deepest centre encountered during transit (Schmidlin 1977). Also, since the carrier requires less free time to cross the specimen at high fields than at low ones, the dividing energy between 'shallow' and 'deep' traps tends to move upwards as the field increases. The degree of thermalization during transit is determined by free-carrier *trapping* ballistics; the criteria for which are assumed not to be significantly temperature dependent. Thus, the activation energy of the mobility at a particular field provides a reasonable indication of the maximum depth E_m to which shallow trapping has occurred (Marshall and Allen 1979). To obtain an approximate value for the density of localized states at this energy, we recall that, if the transit time is comparable to the release time constant for traps at E_m, then carriers have necessarily been trapped only once during transit in these rate-limiting centres. Therefore, the *free*-carrier transit time must be approximately equal to the trapping time into states close to (i.e. within about kT of) E_m, giving

$$\tau_{free} \sim 1/[N(E_m)kTv_{th}\sigma], \tag{2}$$

where v_{th} is the thermal velocity of the carriers, and σ is the capture cross-section of the

trapping centres. Also, τ_{free} is inversely proportional to the applied electric field, F

$$\tau_{free} = w/(\mu_0 F), \tag{3}$$

where w is the width of the specimen film. Combining eqns. (2) and (3), and assuming an energy-independent capture cross-section, the density of states at energy E_m is readily seen to be in approximately linear proportion to the applied field corresponding to this mobility activation energy

$$N(E_m) \propto F. \tag{4}$$

Figure 3 (*a*) displays the (relative) density of states computed from the data of fig. 2 using the above method (open circles). $N(E)$ falls to a low value close to 0·15 eV, as anticipated from the asymptotic behaviour of the mobility activation energy at low fields.

Application of an expression similar to eqn. (1) provides an alternative procedure for determining the ratio $N(E)/N_c$ (Marshall and Allen 1979). The computed values, taking μ_0 as $20\,cm^2\,V^{-1}\,s^{-1}$ as indicated by the approach to high-temperature

Fig. 3

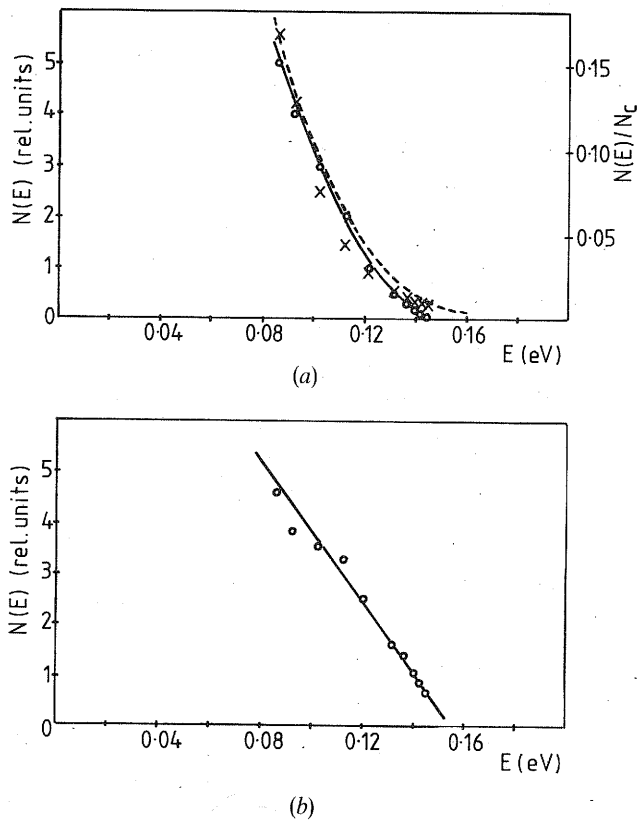

Computed energy distributions of localized states, as obtained using (*a*) eqn. (4) (open circles) and eqn. (1) (crosses); and (*b*) eqn. (5). The dashed line in fig. 3 (*a*) indicates the energy distribution previously employed by Street (1985).

saturation in this and other studies, are presented in the table, and are shown as crosses in fig. 3 (*a*). There is a good general agreement with the results obtained using eqn. (4), and, although the method is intrinsically less accurate (requiring extrapolation of $1/T$ to zero in order to determine $N_c/N(E_m)$), its fixing of the vertical scale is a valuable feature in that it permits an assessment of the capture cross-section (see below). Interestingly, an energy distribution which is very similar to that of fig. 3 (*a*) (including the scaling relative to N_c) has previously been proposed by Street (1985), on the basis of various studies at Xerox and elsewhere. This is indicated by the dotted line in the figure.

Recent work (Marshall and Berkin 1986) has identified certain limitations of the techniques employed above for the computation of the energy distribution of localized states. A re-appraisal of the thermalization process, taking better account of the distinction between shallow and deep traps, leads to the expression

$$N(E_m) \propto -\mathrm{d}F/\mathrm{d}E. \tag{5}$$

Using this procedure, the computed density of states still approaches zero at about 0·15 eV, but the variation with energy now becomes almost linear over the full 0·08–0·15 eV accessible range of energy (fig. 3 (*b*)). Interestingly, if we apply the density scale on the right hand side of fig. 3 (*a*), the data extrapolate to about $0{\cdot}4N_c$ at zero energy. Within the accuracy of the calculations, this implies an almost linear variation of $N(E)$ from the mobility edge down to 0·15 eV. Beyond this extremity, the $N(E)\sigma$ product must be sufficiently low as to prevent further thermalization.

In addition to providing information concerning the energy distribution of localized states, the time-of-flight measurements for the low-temperature anomalously-dispersive regime allows an estimation of their capture cross-sections. Having determined $N(E)$ via application of eqn. (1) (crosses in fig. 3 (*a*)), we may use eqns. (2) and (3) to determine σ. For this purpose, we again take μ_0 as 20 $\mathrm{cm^2\,V^{-1}\,s^{-1}}$, and assume N_c to be of order 10^{20} $\mathrm{cm^{-3}}$. The results are as indicated in the table. For fields in the range 5×10^3–5×10^4 $\mathrm{V\,cm^{-1}}$, values are essentially constant at 1×10^{-17} $\mathrm{cm^2}$. At lower fields, there is a trend towards smaller values, which may well reflect limitations in the computational procedure. In calculating the cross-section, we assume only one trapping event per transit in the dominant states. However, at low fields the carriers have time to approach the bottom of the band tail, so that thermalization is more complete. If, in reality, a carrier crossing the specimen at low fields should experience several trapping events in centres within kT of the tip of the tail, this would certainly give rise to a reduction in the estimated cross-section, as observed.

Taking into account that the appropriate value for N_c might be in the range 10^{19}–10^{20} $\mathrm{cm^{-3}}$, the overall magnitude of the computed capture cross-sections will be 10^{-16}–10^{-17} $\mathrm{cm^2}$. Such a value is typical of centres which are neutral when empty, as expected for states forming the conduction-band tail.

The temperature dependence of the *shape* of the transit pulses shown in fig. 1 provides yet another means for examining the form of $N(E)$. If power-law characteristics are force-fitted to the initial and final decay regimes

$$I(t) \sim t^{-(1-\alpha_1)} \quad \text{(initial regime)} \tag{6a}$$

$$I(t) \sim t^{-(1+\alpha_2)} \quad \text{(final regime)}, \tag{6b}$$

one may compare the parameters α_1 and α_2 with those obtained from computer simulation experiments for various model energy distributions of states (Marshall, Michiel and Adriaenssens 1983).

The data of fig. 1 do not feature exact power-law behaviour in either of the two regimes, and the force-fitted α parameters clearly vary with field in most cases. This is reflected in the spread of values obtained for the experimental data (fig. 4 (*a*)), and is also frequently the case for data from computer simulations. However, it remains possible to establish that the experimental data are closely similar to those for a linear distribution of states (figure 4 (*b*)), and distinctly different from those for other arrays (Marshall *et al.* 1983). In illustration, fig. 4 (*c*) shows the behaviour expected for an exponential tail of states, for which fitted α_2 values tend to be less than or equal to α_1 at all temperatures. Moreover, a comparison of figs. 4 (*a*) and 4 (*b*) yields a tail depth Δ of 0·12–0·15 eV, in very satisfactory agreement with the value determined using the more quantitative (but fundamentally independent) techniques employed above.

Fig. 4

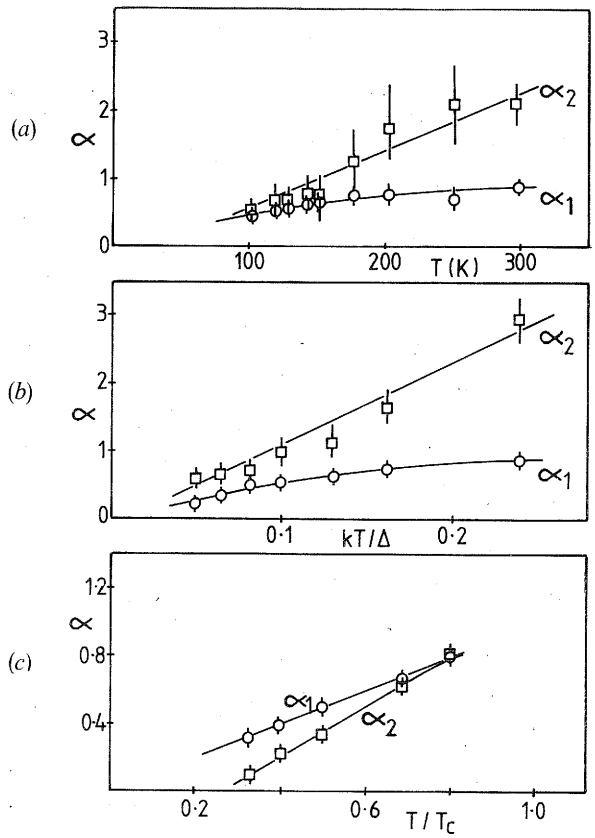

Temperature dependences of the dispersion parameters α_1 and α_2 for (*a*) the experimental study, (*b*) a linear tail of localized states and (*c*) an exponential tail of localized states.

§4. Summary

It has been demonstrated that all of the major features of the time-of-flight data in fig. 1 may be accounted for in terms of interactions between free electrons (having a microscopic mobility of order 20 $cm^2 V^{-1} s^{-1}$) with neutral trapping centres in an approximately linear conduction-band tail of depth close to 0·15 eV. It is also clear that capture by deeper centres constitutes a much weaker process. Unless there is a dramatic

reduction in cross-section from the value of 10^{-17}–10^{-16} cm^2 determined for the tail states, this implies a low ($< 10^{-3} N_c$) background density of localized states for good-quality bulk material. In fact, it has been demonstrated elsewhere (Street 1982) that the deep-tapping lifetime is inversely proportional to the density of dangling-bond centres, suggesting that capture beyond the tail is dominated by these states rather than by any traps at intermediate energies. Therefore, a model involving a band tail of limited extent, plus deeper centres primarily associated with dangling bonds, appears very satisfactory in explaining the transient photo-response characteristics of *bulk* a-Si : H of good quality.

In material of poorer quality, there is a tendency towards lower values of drift mobility and larger activation energies. We associate this with a disorder-induced broadening of the band tail, possibly accompanied by a modification of the density and distribution of deeper states. Similar effects are to be expected close to the surfaces of films, and may well account for observed differences between bulk-dominated and surface-dominated properties. Examples include the fact that mobilities determined in field-effect studies frequently exhibit a smaller magnitude and higher activation energy than is typical of bulk material, and that transient photodecay measurements obtained using coplanar 'surface-cell' specimens indicate a persistence of thermalization over time periods much longer than those found in the present study.

The computed energy distributions of states shown in figs. 3 (*a*) and 3 (*b*) are not dramatically different, the main question being the sharpness of the 'cut-off' close to 0·15 eV. It is possible to use simulation techniques to see which model yields time-of-flight characteristics most closely corresponding to the data of figs. 1 and 2, and we propose to perform such a study in the near future.

Acknowledgment

The authors would like to thank C. Main, H. Michiel and G. J. Adriaenssens for many helpful discussions in connection with this study.

References

Davis, E. A., Michiel, H., and Adriaenssens, G. J., 1985, *Phil. Mag.* B, **52,** 261.
Hourd, A. C., and Spear, W. E., 1985, *Phil. Mag.* B, **51,** L13.
Marshall, J. M., 1983, *Rep. Prog. Phys.*, **46,** 1235; 1985, *J. non-crystalline Solids*, **77/78,** 425.
Marshall, J. M., and Allen, D., 1979, *Phil. Mag.* B, **40,** 71.
Marshall, J. M., and Berkin, J., 1986, *Phil. Mag.* B (to be submitted).
Marshall, J. M., Le Comber, P. G., and Spear, W. E., 1985, *Solid St. Commun.*, **54,** 11.
Marshall, J. M., Michiel, H., and Adriaenssens, G. J., 1983, *Phil. Mag.* B, **47,** 211.
Marshall, J. M., Street, R. A., and Thompson, M. J., 1984 a, *Phys. Rev.* B, **29,** 2331; 1984 b, *J. non-crystalline Solids*, **66,** 175.
Michiel, H., Davis, E. A., and Adriaenssens, G. J., 1985, *J. non-crystalline Solids*, **77/78,** 463.
Mott, N. F., 1969, *Phil. Mag.*, **19,** 835.
Pfister, G., and Scher, H., 1978, *Adv. Phys.*, **27,** 747.
Rose, A., 1951, *RCA Rev.*, **12,** 362.
Schmidlin, F. W., 1977, *Phys. Rev.* B, **16,** 2362.
Spear, W. E., 1968, *J. non-crystalline Solids*, **1,** 197; 1983, *Ibid.*, **59/60,** 1.
Spear, W. E., and Steemers, H. L., 1984, *J. non-crystalline Solids*, **66,** 163.
Street, R. A., 1982, *Appl. Phys. Lett.*, **41,** 1060; 1985, *J. non-crystalline Solids*, **77/78,** 1.
Street, R. A., Knights, J. C., and Biegelsen, D. K., 1978, *Phys. Rev.* B, **18,** 1880.
Street, R. A., Zesch, J., and Thompson, M. J., 1983, *Appl. Phys. Lett.*, **43,** 672.
Tiedje, T., 1984, *Semiconductors and Semimetals*, Volume 21, Pt. C, edited by J. I. Pankove (New York: Academic Press).
Tiedje, T., Cebulka, J. M., Morel, D. L., and Abeles, B., 1981, *Phys. Rev. Lett.*, **46,** 1425.